LABORATORI NAZIONALI DI FRASCATI
SIS – Pubblicazioni

LNF-97/005 (P)
5 Febbraio 1997

The Gravitational Wave Detector NAUTILUS Operating at T=0.1 K

P. ASTONE[1], M. BASSAN[2], P. BONIFAZI[3], P. CARELLI[4], E. COCCIA[2], C. COSMELLI[1], V. FAFONE[2], S. FRASCA[1], A. MARINI[5], G. MAZZITELLI[5], Y. MINENKOV[2], I. MODENA[2], G. MODESTINO[5], A. MOLETI[2], G.V. PALLOTTINO[1], M.A. PAPA[2], G. PIZZELLA[2,5], P. RAPAGNANI[1], F. RICCI[1], F. RONGA[5], R. TERENZI[3], M. VISCO[3], L. VOTANO[5]

[1]Dipartimento di Fisica, Universita` di Roma "La Sapienza" and INFN Sezione di Roma
[2]Dipartimento di Fisica, Universita` di Roma "Tor Vergata" and INFN Sezione di Roma 2
[3]Istituto di Fisica dello Spazio Interplanetario, CNR, Frascati and INFN Sezione di Roma
[4]Dipartimento di Fisica, Universita` dell'Aquila and INFN Sezione dell'Aquila
[5]INFN Laboratori Nazionali di Frascati

ABSTRACT

We report on the ultralow–temperature resonant–mass gravitational–wave detector NAUTILUS, operating at the Frascati INFN Laboratories. The present aim of this detector is to achieve a sensitivity sufficient to detect bursts of gravitational radiation from sources located in our Galaxy and in the local group. Progress in transducer technology is likely to lead to sensitivities that will enable us to observe events from sources as far away as the Virgo cluster of galaxies. We describe the cryogenic apparatus, readout system, cosmic–ray veto system, and give first results obtained during one year of continuous operation at T=0.1K. In particular the Brownian noise of the detector at T=0.1 K was measured. The measured strain sensitivity was $\tilde{h} \approx 6\ 10^{-22}\ \mathrm{Hz}^{-1/2}$ at the frequencies of the two modes, 908 Hz and 924 Hz, with bandwidths of about 1 Hz.

PACS n.: 04.80.+z

To be published on Astroparticle Physics

1. INTRODUCTION

The gravitational wave (GW) detector first developed by Weber [1] and subsequently adopted by other experimental groups [2,3] consists of a carefully suspended body whose vibrational normal modes having a mass quadrupole moment, such as the fundamental longitudinal mode of a cylindrical bar, can be excited by a GW with nonzero energy spectral density at the mode eigenfrequency, which is typically chosen to be about 1 kHz.

The mechanical oscillation induced in the antenna by interaction with the GW is transformed into an electrical signal by a motion or strain transducer and then amplified by an electrical amplifier. Unavoidably, brownian motion noise associated with dissipation in the resonant mass, and electronic noise from the amplifier, limit the sensitivity of the detector.

Typically the detector output is filtered by a suitable linear filter that is designed to optimize the signal–to–noise ratio to particular signals[4–6].

Sources of GWs for resonant–mass detectors can be divided into three groups, according to the spectral character of the signal produced[7]:

- burst sources: collapsing and bouncing of supernovae cores, coalescence of compact binary system, births of black holes, collisions between black holes and between black holes and neutron stars, star quakes in neutron stars, and speculative sources, such as the coalescence of a population of compact MACHO's in the galactic halo [8,9].
- continuous sources: rapidly rotating (millisecond period) deformed neutron stars.
- stochastic sources: fluctuations in the density of the early universe, backgrounds based on cosmological string models [10].

The sensitivity of a resonant–mass detector can be given in term of the spectral density of strain $S(f)$, or its square root $\tilde{h}$ (the spectral amplitude). $S(f)$ represents the input GW spectrum that would produce a signal equal to the noise spectrum actually observed at the output of the antenna instrumentation. In a resonant–mass detector, this function is a resonant curve and can be characterized by its value at resonance $S(f_0)$ and by its half height width Δf. $S(f_0)$ can be written as [11]:

$$S(f_0) = \frac{\pi}{2}\frac{kT_e}{Mv_s^2 Qf_0} \tag{1}$$

here T_e is the thermodynamic temperature of the detector, T, plus a backaction contribution from the amplifier, which is very small for the present readout system, M is the mass of the bar, v_s is the speed of sound of the bar material, and Q is the quality factor of the mode. The half height width of $S(f_0)$ gives the bandwidth of the resonant mode:

$$\Delta f = \frac{f_0}{Q}\Gamma^{-1/2} \tag{2}$$

where Γ is the spectral ratio between electronic and brownian noise [11] (usually $\Gamma \ll 1$):

$$\Gamma = \frac{T_n}{\beta Q T_e} \tag{3}$$

T_n is the amplifier noise temperature and β the coupling parameter of the transducer to the bar.

The eqs. (1) and (2) characterize the sensitivity of a resonant–mass detector. The optimum performance of the detector is obtained by filtering the output with a filter matched to the signal. The energy signal–to–noise ratio of the filter output is given by [12]:

$$SNR = \int_{-\infty}^{+\infty} \frac{|H(f)|^2}{S(f)} df \qquad (4)$$

where $H(f)$ is the Fourier transform of the signal waveform $h(t)$.

The detector sensitivity to short burst can be expressed as the minimum detectable (SNR=1) GW Fourier component at the resonant frequency, can be easily calculated from eq. (4) and is usually written as:

$$H_{min}(f_o) = \frac{L}{\nu_1^2} \sqrt{\frac{kT_{eff}}{M}} \qquad (5)$$

where L is the bar length and T_{eff} is the detector effective noise temperature, representing (in Kelvin) the minimum detectable energy innovation:

$$T_{eff} \cong 4T\Gamma^{1/2}$$

In order to express the sensitivity in terms of the dimensionless GW amplitude $h(t)$, we need to make assumptions on the GW spectrum. If, conventionally, we assume a flat spectrum from 0 to f_g, as roughly expected from a featureless waveform of amplitude h and duration $\tau_g \approx f_g^{-1}$, much smaller than the detector damping time, then $h_{min} \approx H_{min}/\tau_g$.

Several resonant–mass detectors, cooled to liquid helium temperatures, are monitoring, since several years, the strongest potential sources in our Galaxy [13]. Cryogenic operation, superconducting electronics, improved vibration isolation and increased acoustic Q–factors have contributed to a 10^4 fold improvement in energy sensitivity over Weber's original antennas. Three such detectors (Stanford, ALLEGRO at LSU, EXPLORER at CERN) already in 1986 set an upper limit on the intensity of GW bathing the Earth[14]. In 1989 EXPLORER, cooled to 2.0 K with superfluid helium, reached a sensitivity $h \approx 7\ 10^{-19}$ [15], soon followed, at this sensitivity level, by ALLEGRO[16] and then by the Perth detector NIOBE'[17]. The expected rate of event is of the order of 1 per 10 years. Much higher rate (many events per year) could be get by extending the observable range to the Virgo cluster of galaxies. These events would cause a strain in a resonant bar of the order of $h \approx 3\ 10^{-21}$, which means an energy captured by the antenna as low as 10^{-31} J, corresponding to an effective noise temperature of the order of 10^{-7} K. In terms of vibrational energy this is equivalent to one phonon.

It can be demonstrated that in the limit of very low $T/\beta Q$ the effective noise temperature is bound to the amplifier noise temperature, which for any linear amplifier has a fundamental limitation: kT_n cannot be less than $\hbar\omega$ because of the uncertainty principle[5] ($T_n \geq \hbar\omega_a/k \approx 10^{-7}\,K$). Sensitivity at the single–phonon level is referred to as the standard quantum limit. The achievement of a quantum–limited macroscopic oscillator is the challenge of

the future resonant–mass detectors. To reach this goal, the experimental parameters determining the detector sensitivity must be pushed to the extreme limit of existing technology.

A fundamental step in this direction is represented by two new generation detectors, designed to operate at a thermodynamic temperature of about 100 mK, which have been constructed in Italy: NAUTILUS [18], at Frascati INFN Natl. Labs, and AURIGA [19], at Legnaro INFN Natl. Labs.

The NAUTILUS program started with the feasibility study of the cooling below 0.1 K of a large, high–Q aluminium mass [20]. It was planned to develope a resonant capacitive transducer [21] with large β and a dc SQUID amplifier [22] with noise temperature as near as possible to the quantum limit. The detector, constructed in Italy, was assembled and tested to ultralow temperatures in the CERN laboratories [23], and then moved to Frascati, where, after an intense setting up period, is now operating.

2. THE CRYOGENIC APPARATUS

The layout of the NAUTILUS cryogenic apparatus is shown in fig. 1. The most important feature of the cryostat is its central section, which is shorter than the cylindrical Al 5056 bar antenna (hereafter indicated as the bar) of mass 2350 kg, length 3.0 m, and diameter 0.6 m. The central section contains:

– two aluminum alloy shields cooled by helium gas,
– a stainless steel liquid helium (LHe) reservoir (2000 liters capacity),
– three massive copper rings,
– a special ^{3}He–^{4}He dilution refrigerator [24–26], through the top central access.

End caps are fastened to each stage of the cryostat to complete the seven shields surrounding the bar. The shields are suspended one from the other, forming a cascade of low–pass mechanical filters. The attenuation of each individual filter has been measured and is reported in table 1.

The bar suspension and the thermal link to the refrigerator were defined after experimental tests on various solutions [27]. We adopted a U–shaped (Weber type) oxygen–free high–conductivity (OFHC) copper cable, wrapped around the bar central section and hung from the central ring of the innermost shield of the cryostat. This cable suspension also provides the necessary thermal path between the refrigerator thermal contacts and the bar.

The internal copper shield hangs from the intermediate copper shield by means of two U–shaped titanium rods (alloy Ti64). The middle shield is suspended from the external shield by four Ti64 cables with intermediate lead masses. The liquid helium vessel and the two external shields cooled by the helium gas are suspended by four Ti64 cables, hung at room temperature to a stack of 8 rubber and steel disks.

The overall mechanical vibration isolation at the bar resonant frequency (about 900 Hz) is about –260 dB. In order to eliminate the acoustic noise from the boiling liquid helium, the helium bath is kept in a superfluid regime, at a pressure of about 20 mbar.

The external copper shield is thermally anchored to the 1 K pot of the refrigerator. The intermediate and inner shields are in thermal contact with the two step heat exchangers of the dilution refrigerator; the mixing chamber [26] is in thermal contact with the ends of the bar suspension cable. Here the thermal path is provided by soft multiwire copper braids, in order to minimize the transmission of mechanical vibration to the bar (see fig. 2).

The dilution refrigerator cooling power is shown in fig. 3. The mixture is circulated by a roots blower (1000 m^3/h) and a primary rotary pump (120 m^3/h), both leak tight. A similar pumping system is used for the 1 K pot.

The thermal behaviour of the cryostat is monitored by a thermometry system, designed to monitor the cooling of each shield and of the antenna from room temperature down to the millikelvin region. A total of 20 GaAs diodes are used to measure the temperature of the two helium gas shields and of the liquid helium reservoir. In the experimental vacuum, each one of the copper shields is monitored by a GaAs diode in order to measure the temperature down to 1.5 K, and by two calibrated Ge thermometers, one at the center and the other at the end of one of the caps, to measure the thermal gradients. Each one of these Ge thermometers is connected to the readout instrumentation by high resistivity constantan wires, which are clamped on the surface of each shield by copper strips. This technique provides good thermal sinking and electromagnetic shielding of the sensors. The antenna itself is equipped with one Ge and one diode thermometer in the central section and one Ge sensor on the end face where also the transducer is located. Both Ge sensors are inserted in carefully calibrated holes made in the cylindrical bar to ensure a good thermal contact.

Figure 4 shows the bar temperature during a typical cooldown. About three weeks are needed to reach 77 K, using 8000 liters of liquid nitrogen, and about one week to achieve 4.2 K, using about 5000 liters of LHe. The 1 K pot is then filled with LHe at low pressure and the ^3He–^4He mixture condense and circulated in the dilution refrigerator. After a few days, the calibrated Ge thermometer indicates a temperature of about 90 mK on the bar end face and 45 mK on the mixing chamber. As far as we know, the NAUTILUS detector was the first massive body cooled to these very low temperatures.

The characteristics of the cooling agree with those of an early model [25]. From the measured thermal gradient between the mixing chamber and the bar end (about 30 mK) we deduce an upper limit of 10 μW for the antenna heat leak (corresponding to 1.7 μWm^{-2}).

Figure 5 shows the temperature of the inner copper shields during cooldown. The overall LHe evaporation rate at regime is about 90 liters/day (40 from the helium reservoir and 50 from the 1K pot).

In order to operate the detector , the pressure of the residual gas in the antenna vacuum must be lower than 10^{-5} mbar; otherways, the capacitive transducer (see below) cannot be biased with the necessary dc voltage. The bar has two stable equilibrium temperatures: about 100 mK, if the refrigerator is in full operation, and about 1.3 K, if just a very low flow is mantained in the refrigerator, which then acts as a good thermal link to the 1 K pot.

3. READOUT SYSTEM

The configuration of the electronic instrumentation of NAUTILUS (see fig. 6) is similar to that developed for the EXPLORER detector; we address the reader to ref. 15 for technical details. We recall here that the vibrations of the bar are converted into electrical signals by a capacitive transducer resonating at the antenna frequency in order to improve the energy transfer from the bar to the electronics. The signals are applied to the input coil of a dc SQUID amplifier by means of a superconducting transformer, which provides the required impedance matching.

The capacitive transducer bolted to one end of the antenna consists of a vibrating disk with mass M_t=0.32 kg and of a fixed plate with a gap of d= 49 μm and total capacitance C_t=3.95 nF.

The transducer and the bar form a system of two coupled oscillators which are perfectly coupled when the transducer biasing voltage is 310 V, since the frequency f_t of the lowest symmetrical flexural mode of the transducer is then very close to that of the first longitudinal mode of the bar f_b. The frequencies (f_- and f_+) of the resulting normal modes are spaced by about $f_a\mu^{1/2}$, where $\mu=2.42 \times 10^{-4}$ is the ratio between the effective masses of the transducer disk and the bar.

The high–impedance transducer is connected to the low–inductance (L_{in} = 1 μH) input coil of the SQUID through a decoupling capacitance (C_d = 100 nF) and a superconducting transformer with a high turn ratio (N=1270), primary inductance L_o = 2.86 H, secondary inductance L_i=0.8 μH, and coupling factor k_c=0.8. The electrical circuit exhibits a resonance at f_{el} = 1780 Hz, so we have a third (electrical) mode, which is, however, only very weakly coupled to the mechanical modes.

The dc SQUID is a planar device with a multiloop geometry having very low intrinsic noise and good coupling to the external world [21]. The device is biased with a dc current (about 40μA) and an ac modulation flux at f_m=90 kHz applied through a coil and is operated in the flux–locked loop configuration. Its output signal is applied to a low–noise differential FET amplifier through a cooled LC resonant circuit (Q=70) tuned at f_m (tank circuit), which provides the proper noise impedance matching. The FET amplifier is followed by a lock–in amplifier, driven at f_m, whose output V(t) is fed back to the SQUID via a weakly coupled coil in order to stabilize its operating point and to linearize its input–output (V/ϕ) characteristics. The gain of the SQUID amplifier is continuously monitored by means of a calibrated reference signal of known flux amplitude ϕ_c applied to the SQUID at a frequency f_c, between the frequencies of the two modes, through an additional coil. The corresponding output signal is used to normalize the data during the analysis. The main features of the detector are resumed in table 2.

The output signal from the SQUID instrumentation is directly sent to the acquisition system as well as to four lock–in amplifiers, which extract the Fourier components at the mode frequencies (f_-, f_+), calibration flux frequency (f_c), and in the region between the modes (f_{wb}) to obtain information on the detector wide–band noise. The use of a lock–in amplifier at each frequency f_- and f_+ allows one to demodulate the signal in a bandwidth defined by the integration time t_o=0.3 s of the instrument. Both the outputs of the two–phase lock–in amplifier, i.e., the "in phase" and "quadrature" components $p(t)$ and $q(t)$, are needed to reconstruct the signal amplitude. The signal energy $E(t)$ is proportional to $r^2(t) = p^2(t) + q^2(t)$.

For calibrating the detector we can use two devices: a) a second capacitive transducer, mounted at the opposite end of the bar; b) a piezoelectric (pzt) ceramic glued on the bar surface near the central section. The calibrator a) can be used for exciting the first longitudinal mode of the bar with a given known force. It can be also used, being tuned at the bar second longitudinal mode frequency, to monitor the second harmonic vibrations, thus providing a veto for non GW signals.

We have actually calibrated the antenna using the pzt. After measuring the pzt coupling constant, we applied a wave packet of short duration to the pzt. We then compared the measured pulse energy at the output of the SQUID instrumentation with that computed from the knowledge of the equivalent circuit of the detector. With signals of the order of 5 10^6 K, we found a ratio computed/experimental of 1.3 for the – mode and of 1.4 for the + mode.

4. ACQUISITION AND DATA ANALYSIS

The data–acquisition system is based on a VAX 3800 minicomputer, which is connected to the INFN network and can be remotely operated. This machine performs the acquisition and permanent recording of the data in a suitable form for further off–line analysis as well as various functions of on–line analysis for diagnostic purposes.

The data are analyzed using three different techniques: the standard Wiener filter with fixed parameters (on line); an adaptive Wiener filter (off line)[28], which accounts for the nonstationary nature of the noise, thereby improving the sensitivity; and an adaptive matched filter (both on–line and off–line) [29, 30] operating on the signal directly sampled at the output of the SQUID instrumentation.

Analog–to–digital conversion and acquisition of the data are performed inside the VAX by an ADQ32 card with 32 input lines (see table 3). The first 12 channels (except channel 6) are subsampled before being recorded with sampling time $\Delta t = 0.29$ s (slow sampling). Channel 6, called "direct acquisition" and used for the matched filter, provides the antenna signal taken before the lock–in amplifiers, which is recorded at the rate of 110 Hz (fast sampling). We also have slow channels, recorded every 29 s, to monitor the behaviour of the cryogenic system (temperatures, pressures, levels and flows of the cryogenic liquids).

Each block of recorded data contains the timing information, which is obtained by combining the data from a GPS device and a radio receiver tuned to a standard–time broadcasting station.

The software also has monitoring and diagnostic facilities for operating the detector. All the results (statistics, time histories, distributions and spectra) of the recorded data and the filtered data (see above) can be displayed, thereby providing a powerful diagnostic tool for managing the experiment.

5. VETOES

NAUTILUS has been equipped with a cosmic–ray veto system [31] consisting of layers of streamer tubes [32] placed above and below the antenna cryostat. A cosmic rays detector is necessary because extensive air showers (EAS) or energetic single particles (muons or hadrons) interacting in the antenna may produce detectable signals whose rate increases with increasing sensitivity of the antenna [33–35]. For instance, with a sensitivity of $T_{eff} \sim 1$ mK, about two cosmic–ray events per day are expected, but the rate increases to about $5\ 10^3$ if the quantum limit is reached.

The cosmic–ray detector has a modular structure that facilitates disassembly during the GW detector maintenance operations. The detector consists of seven layers of limited streamer tubes (LSTs), three (6x6 m^2, 24 LSTs each) mounted above the cryostat and four layers (6x2.75 m^2, 11 LSTs each) placed at ground level (see fig.1). The LSTs are 6–m–long large–size coverless plastic tubes operating in the limited streamer regime. The analog readout of the LST wires allows one to measure the multiplicity of the particles impinging on the detector.

The trigger logic is designed for detecting high–energy muons and hadrons interacting in the antenna as well as EAS. Three different triggers can be selected. The first (μ trigger) is used for a periodic calibration of the system. The second (interacting particle trigger) selects those events in which one or more particles interact with the gravitational wave detector; the trigger rate is about 2 Hz. The third (neutral particle trigger) requires that no particles cross the top

module, while more than 20 particles cross the bottom module (the rate is about 2 Hz). It should detect neutrons interacting in the bar or the large–angle charged particles that do not cross the upper telescope.

The cosmic–ray veto system has demonstrated good performance, well up to the physics requirements of the experiment and the simulation results.

The experimental apparatus includes others vetoes, such as a vibration sensor (accelerometer) and a magnetic–field sensor (search coil) both located on the cryostat, which monitor the laboratory environment. Another signal used as a veto is the output of the antenna seen through the SQUID instrumentation and bandpass filtered between 20 and 70 Hz, a region where some resonances of the suspension system may be observed.

6. EXPERIMENTAL RESULTS

The NAUTILUS detector had a first run of data taking from December 1994 until June 1995. In this run we had a major problem of a non–stationary noise excess due to an up–conversion mechanism likely acting on the last stages of the suspension system. For this reason NAUTILUS was warmed up on July 1995, in order to make some changes in the suspension system for a more stable position setting. A second run is underway since December 1995. The main results so far collected are resumed below.

- In the one–year period December 1995 to December 1996 the detector temperature was continuously at 0.1 K, except during few interruptions for manteinance and for the repairing of a pump. The thermal duty cycle was of about 85%. This is the first reported long term operation of a large massive body at ultralow temperature.

- In fig. 7 we show the experimental strain sensitivity of the detector. The quantity plotted is the GW spectral amplitude $\tilde{h}$ [$Hz^{-1/2}$]. There are maxima sensitivities at about 908 Hz (f_-) and 924 Hz (f_+) where we could measure with SNR=1 a spectral amplitude $\tilde{h} \approx 6\ 10^{-22}$ $Hz^{-1/2}$. The half–heigth bandwidths are of about 1 Hz. However, it is interesting to note that the spectral amplitude is better than $2\ 10^{-20}$ $Hz^{-1/2}$ in a total bandwith of about 25 Hz. New upper limits on a stochastic background of GW could be obtained with two detectors at this sensitivity [11].

- In fig. 8 we show the detector amplitude distribution of three hours of data filtered with an optimum matched filter. The bar thermodynamic temperature was 0.1 K. The experimental data are in very good agreement with a gaussian distribution, whose variance directly gives T_{eff}= 4.1 mK. This corresponds to a millisecond GW burst amplitude $h_{min}=5\ 10^{-19}$.

- In fig. 9 we show a Brownian noise measurement. We report the detector energy *E(t)* in a period lasting about 3 hours, and the relative distribution. The contribution to the measured average value due to the wideband noise ($\Phi_n \approx 5\ 10^{-5}\ \Phi_o Hz^{-1/2}$) is of about 10 mK, while the effect of the SQUID backaction is estimated to be less than 10 mK. The reported average value is in agreement with the detector thermodynamic temperature (T=110 mK), as measured by a calibrated germanium thermometer located at one end of the bar. To our knowledge this is the first time that such a low temperature is measured by using the Brownian noise of a mechanical oscillator.

- We report preliminary results of the search for coincidences between the GW and cosmic–ray detectors, during a period of 130 hours in which the hourly average of the experimental T_{eff} was less than 20 mK, during the first months of 1996. A lower energy threshold of 100 mK was applied to the GW detector data processed with the adaptive Wiener filter. We used a +/– 1 s coincidence time window and considered two samples of cosmic–ray events: a) EAS selected with the requirement of more than 50 particles/m^2 on the top module; b) single interacting particles with the requirement of zero or one particle in the top module and more than 500 particles in the bottom module. For a) we found zero coincidences with an expected number of accidentals $<n>_{acc}=2.4$, corresponding to an upper limit at 90 % CL of 0.7 concidences per day; for b), 11 coincidences with $<n>_{acc}=8.2$, corresponding to an upper limit at 90% CL of 1.6 coincidences per day. The $<n>_{acc}$ is obtained experimentally by random changes of the occurence times of the cosmic rays.

These are the first results of the cosmic–ray (hadrons, muons, and EAS) effects on a cryogenic antenna at sea level [36]. At Stanford [33] only EAS events were considered, and the detector was under 1 meter of concrete shielding. From the Montecarlo simulation, at energies above 100 mK, we expect about 10^{-2} events/day to give detectable signals in the antenna. Hence, higher statistics and better sensitivity are required in order to reach a significant excess of coincidences. Data are being collected.

NAUTILUS is at present in continuous data taking. The detector duty cycle is limited to 85% by cryogenic operations. The percentage of time during which the detector can see with SNR>1 a gravitational collapse with 10^{-3} solar masses converted in a millisecond GW burst at Galactic center is of about 60%. We know we can increase the sensitivity, by solving residual non stationary noise excess problems. We are studing these residual effects.
Improvements in the transducer (small–gap design) and dcSQUID amplifier (higher coupling with the input coil), as well as the implementation of the high–frequency data acquisition and on–line analysis system, are currently underway in parallel to the detector operation. We plan to reach in a few years $T_{eff}=10\mu K$, and to be sensitive to a GW spectrum of the order of $\tilde{h}\approx 5\ 10^{-23}\ Hz^{-1/2}$ over a bandwidth of the order of 10 Hz.

Aknowledgements

The NAUTILUS detector is funded by the Istituto Nazionale di Fisica Nucleare (INFN). The full support of Enzo Iarocci has been essential for the installation of this experiment in Italy. We thank Franco Bronzini for his contribution to the design of the cryogenic apparatus and Piero Benvenuto, Domenico Fabbri, Gianni Federici, Giancarlo Martinelli, Eugenio Serrani, Roberto Simonetti and Maurizio Ventura for their continuous technical support. We express our thanks to Bruno Dulach and Sergio Faini for their support during the installation of the detector at LNF and to the personnel of the LNF Cryogenic Facility for the efficient supply of cryogenic liquids.

References

[1] J. Weber Phys. Rev. 117, 306 (1960).

[2] E. Amaldi and G. Pizzella in *Relativity. Quanta and Cosmology in the development of the scientific thought of Albert Einstein*, Johnson Reprint Corporation (Academic Press, New York, 1979)

[3] K.S. Thorne in *Three hundred years of gravitation*, S.W. Hawking and W. Israel editors (Cambridge University Press, 1987).

[4] GW Gibbons and S.W. Hawking, Phys. Rev D 14, 2478 (1976).

[5] R.P. Giffard, Phys. Rev. D14 2478 (1976).

[6] G.V. Pallottino and G. Pizzella, Il Nuovo Cimento C4, 237 (1981).

[7] M.Rees, R. Ruffini and J.A. Wheeler, *Black holes, Gravitational Waves and Cosmology* (Gordon and Beach, New York, 1974).

[8] M.S. Turner, E.I. Gates and G.Gyuk, preprint Fermilab–Pub 96/022–A.

[9] L.S.Finn, to appear on the Proc. of the Workshop OMNI 1, San Jose dos Campos (Brasil) 1996, World Scientific.

[10] R. Brustein, M Gasperini, M. Giovannini, and G. Veneziano, Phys. Lett. B 361,45 (1995)

[11] P. Astone et al. Phys. Lett. B 385, 421 (1996)

[12] P. Astone, A. Lobo and B. Schutz, Class. and Quantum Grav. 11, 2093 (1994)

[13] Gravitational Wave Experiments, Proceedings of the First Edoardo Amaldi Conference, Frascati 1994, edited by E. Coccia, G. Pizzella and F. Ronga (World Scientific, Singapore, 1995)

[14] E. Amaldi et al., Astron. Astrophys. 216, 325 (1989).

[15] P. Astone et al., Phys. Rev. D47, 2 (1993).

[16] W.W. Johnson et al., in *Gravitational Wave Experiments*, Proceedings of the First Edoardo Amaldi Conference, Frascati 1994, edited by E. Coccia, G. Pizzella and F. Ronga (World Scientific, Singapore, 1995)

[17] D.G. Blair et al., Phys. Rev. Lett. 74, 1908 (1995).

[18] E. Coccia et al., in *Gravitational Wave Experiments*, Proceedings of the First Edoardo Amaldi Conference, Frascati 1994, edited by E. Coccia, G. Pizzella and F. Ronga (World Scientific, Singapore, 1995)

[19] M. Cerdonio et al., in *Gravitational Wave Experiments*, Proceedings of the First Edoardo Amaldi Conference, Frascati 1994, edited by E. Coccia, G. Pizzella and F. Ronga (World Scientific, Singapore, 1995)

[20] E. Coccia, T.O.Niinikoski, Journal of Physics E 16, 695 (1983).

[21] P. Rapagnani, Il Nuovo Cimento C5, 385 (1982).

[22] P. Carelli, M.G. Castellano, C. Cosmelli, V. Foglietti, I. Modena, Phys.Rev. A32, 3258 (1985).

[23] P. Astone et al. Europhysics Letters, 16, 231 (1991).

[24] The dilution refrigerator has been designed and assembled in collaboration with Oxford Instruments Ltd. see also: M.Bassan, E.Coccia, I.Modena, G.Pizzella, P.Rapagnani, F.Ricci in Proceedings of the 5th Marcel Grossmann Meeting on General Relativity, Blair, Buckingham and Ruffini editors (World Scientific, London, 1989).

[25] M. Bassan, E. Coccia, N. Menci, I. Modena, Cryogenics 31 (1991) 147.

[26] E. Coccia and I. Modena, Cryogenics 31 (1991) 712.

[27] E.Coccia, V. Fafone, I. Modena Rev. Sci. Instr. 63 (1992) 5432.

[28] P. Astone et al. Il Nuovo Cimento 15C, 447 (1992).

[29] P. Astone et al. Internal Report 1052, Dipartimento di Fisica, Universita' di Roma "La Sapienza" 1995.

[30] S. Frasca, G.V. Pallottino and G. Pizzella, in Proceedings of the 3rd European Signal Processing Conference, I.T. Young editor (North Holland, Amsterdam, 1986).
[31] E. Coccia, A. Marini, G. Mazzitelli, G. Modestino, F. Ricci, F. Ronga, L. Votano, Nucl. Instr. and Meth. A 355, 624 (1995).
[32] E. Iarocci, Nucl. Instr. and Meth. 217, 30 (1983).
[33] E. Amaldi, G. Pizzella Nuovo Cimento C9 2 (1986).
[34] F. Ricci, Nucl. Instr. and Meth. A260, 491 (1987).
[35] J. Chiang, P. Michelson and J. Price, Nucl. Instr. and Meth. A311, 603 (1992).
[36] P. Astone et al. to appear on the Proc. of the Workshop OMNI 1, San Jose dos Campos (Brasil) 1996, World Scientific.

Table 1 – Attenuation of the various filtering stages of the apparatus.

Load mass	Elastic element of filtering stage	Mean vertical attenuation (dB)
Al5056 bar	Cu rod	–88±5
Cu internal ring	2 U–shaped Ti64 rods	–40±5
Cu middle ring	2 U–shaped stainless steel threads	–40±5
Cu external ring	4 Ti64 cables with intermediate Pb masses	–50±5
Liquid He vessel	4 Ti64 cables + 4x8 rubber disks	–50±5

Table 2 – Main features of the NAUTILUS detector in the first run.

Frequency of the bar (first longitudinal mode)		$f_a = 915.8$ Hz
Mass of the bar		$M = 2260$ kg
Frequency of the transducer (first flexural mode)		$f_t = 924.2$ Hz
Mass of the transducer (disk)		$M_t = 0.32$ kg
Ratio of the two equivalent masses		$\mu = 2.42\ 10^{-4}$
Transducer gap		$d = 49\ \mu$m
Active capacitance of the transducer		$C_t = 3.95$ nF
Stray capacitance of the transducer		$C_0 = 0.91$ nF
Decoupling capacitance		$C_d = 97$ nF
Electrical field in the transducer		$E = 6.4\ 10^6$ V/m
Frequency of the modes	$f_- = 908.343$ Hz	$f_+ = 923.817$ Hz
Merit factors of the modes	$Q_- = 1.26\ 10^6$	$Q_+ = 2.3\ 10^6$
Decay times of the modes	$\tau_- = 440$ s	$\tau_+ = 780$ s
Energy coupling factors	$\beta_- = 3.5\ 10^{-4}$	$\beta_+ = 3.9\ 10^{-4}$
Frequency for the wide-band noise		$f_{wb} = 918$ Hz
Frequency for the SQUID calibration		$f_c = 916.15$ Hz
Transformer primary inductance		$L_0 = 2.86$ H
Transformer secondary inductance		$L_i = 0.8\ \mu$H
Transformer coupling constant		$k_c = 0.8$
SQUID input coil inductance		$L_{in} = 1\ \mu$H
SQUID inductance		$L_s = 5.6$ pH
SQUID coupling factor		$k_s = 0.5$
d.c. SQUID flux noise (one-sided)		$\Phi_n = 5\ 10^{-6}\ \Phi_0/\sqrt{\text{Hz}}$
Modulation frequency of the SQUID		$f_m = 98.1$ kHz
Brownian fluxes (T = 1 K)	$\Phi_- = 8.5\ 10^{-5}\ \Phi_0$	$\Phi_+ = 8.7\ 10^{-5}\ \Phi_0$
Bandwidths	$\Delta f_- = 1.5$ Hz	$\Delta f_+ = 0.85$ Hz

Table 3 – Data acquisition channels and sampling periods.

CH 1	p(t) at f_-	0.2908 s
CH 2	q(t) at f_-	0.2908 s
CH 3	p(t) at f_+	0.2908 s
CH 4	q(t) at f_+	0.2908 s
CH 5	calibration signal at f_c	0.2908 s
CH 6	direct acquisition	4.544 ms
CH 7	wide band noise at f_{wb}	0.2908 s
CH 8	accelerometer 0.2-100 Hz	0.2908 s
CH 9	accelerometer 900-940 Hz	0.2908 s
CH 10	search coil	0.2908 s
CH 11	clock	0.2908 s
CH 12	antenna at low frequency 20-70 Hz	0.2908 s
CH 13	helium bath pressure	0.2908 s
CH 14	helium evaporation flow	0.2908 s
CH 15	isolation vacuum pressure	0.2908 s
CH 16	inner vacuum pressure	0.2908 s
CH 17	pzt on the inner copper shield	0.2908 s
CH 18	1K pot level meter	29.08 s
CH 19	1K pot pressure	29.08 s
CH 20	refrigerator flow	29.08 s
CH 21	mixing chamber temperature	29.08 s
CH 22	antenna temperature	29.08 s

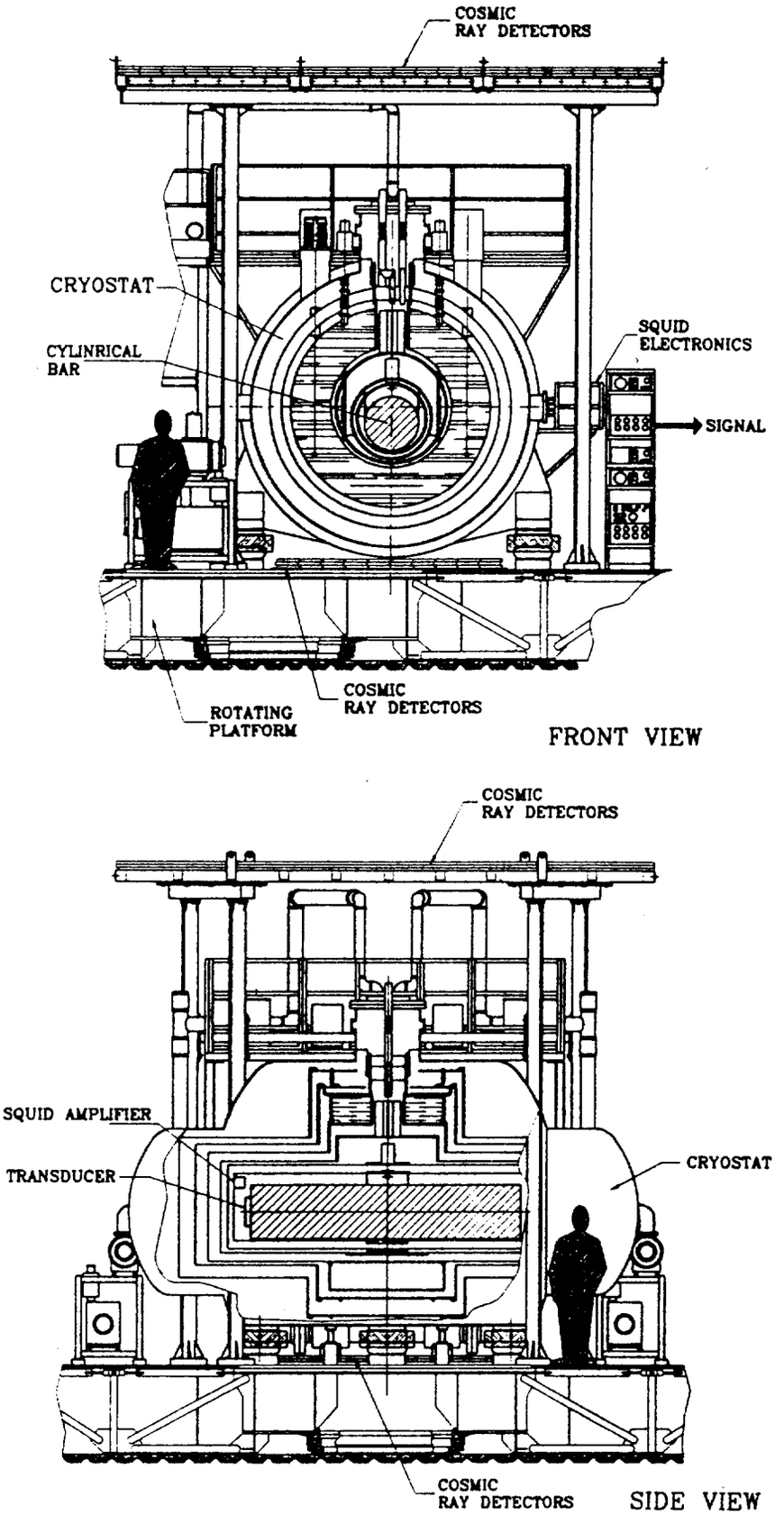

FIG. 1 – Layout of the NAUTILUS cryogenic apparatus.

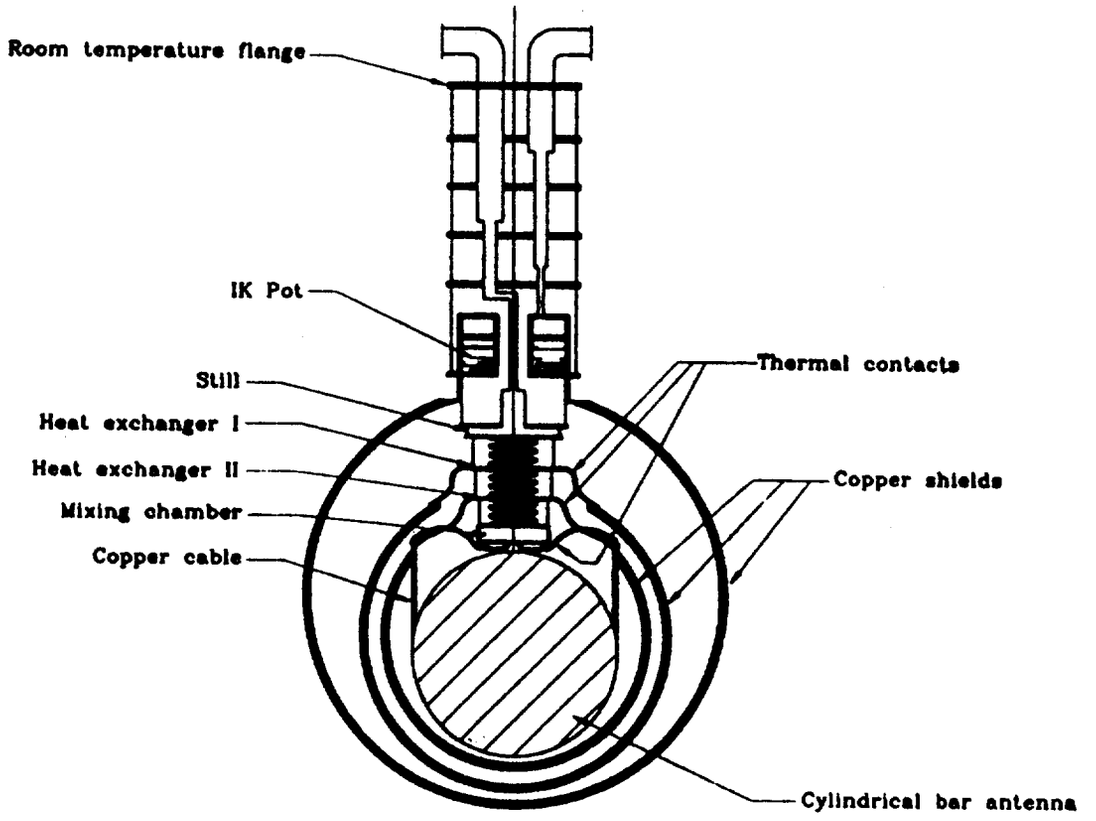

FIG. 2 – Schematic layout of the dilution refrigerator and its connections to the cylindrical bar and to the three copper shields. The shields are suspended to each other and cooled by different stages of the refrigerator. The external shield (2090 kg) is cooled to 1.3 K by the 1K pot; the intermediate shield (860 kg) to about 350 mK by the heat exchanger I; the internal shield (800 kg) to about 180 mK by the heat exchanger II. The bar (2350 kg), is cooled to below 100 mK by the mixing chamber, via the copper cable suspension.

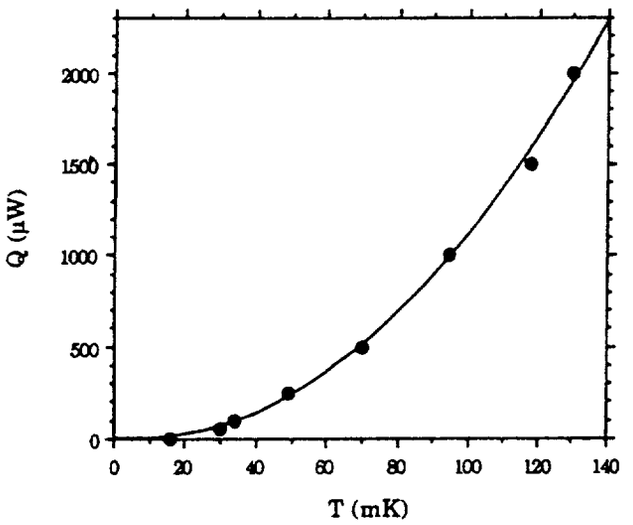

FIG. 3 – Cooling power of the refrigerator. On the ordinate it is reported the heat supplied by an internal heater, on the abscissa the mixing chamber equilibrium temperature.

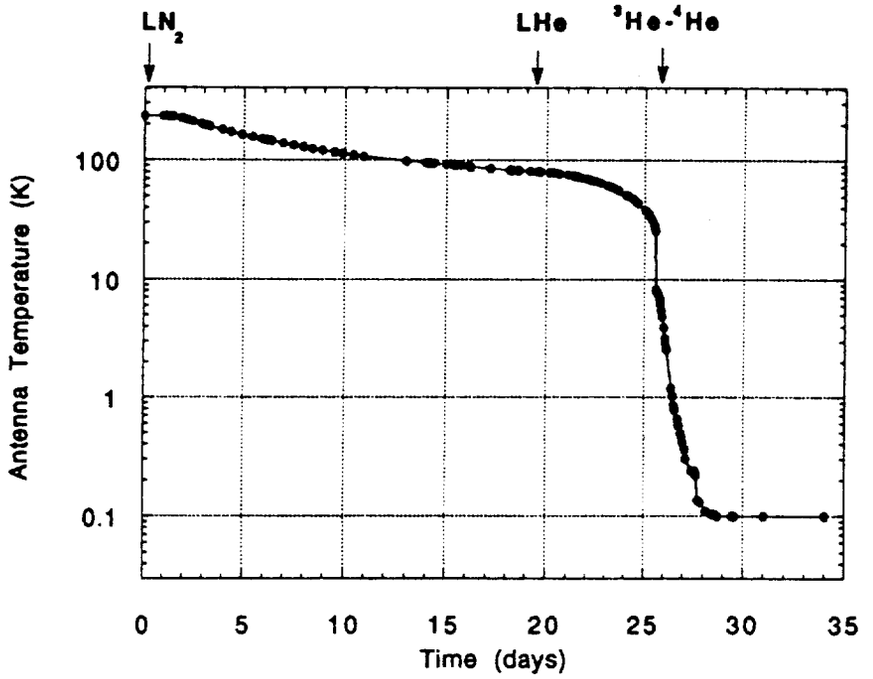

FIG. 4 – Temperature of the cylindrical bar versus time during the cooldown. The arrows indicate the main cryogenic operations, described in the text.

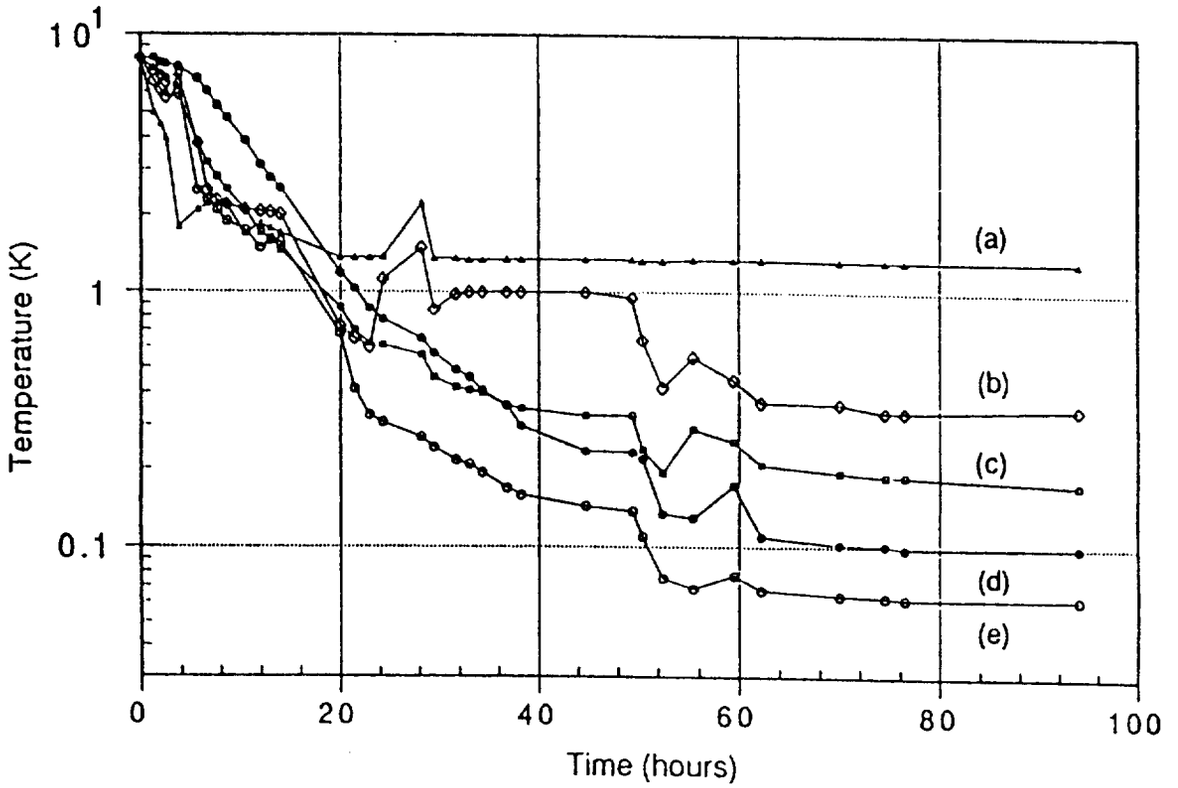

FIG. 5 – Temperatures of the shields during the final phase of the cool down reported in Fig. 4.

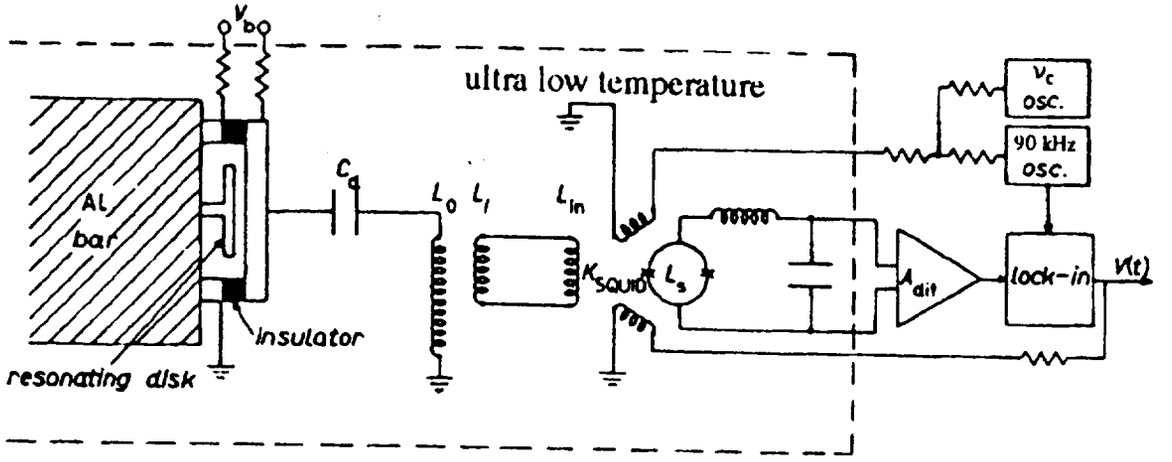

FIG. 6 – Schematic of the electronics of the experimental apparatus. The vibrations of the bar are converted into electrical signals by a resonant capacitive transducer and applied to the SQUID amplifier by a superconducting transformer. The output signals from the SQUID instrumentation contain information on the vibrational state of the antenna and can be properly processed.

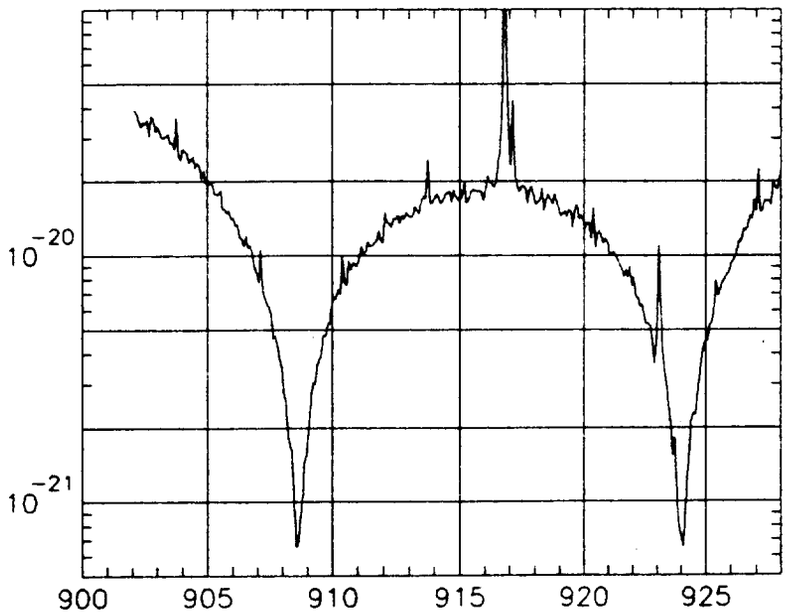

FIG. 7 – Experimental strain sensitivity of the detector (input noise spectral amplitude in units of $Hz^{-1/2}$). The bandwidths of the two peaks at the resonances of the detector are given in table 2. The peak in between corresponds to the calibration reference signal.

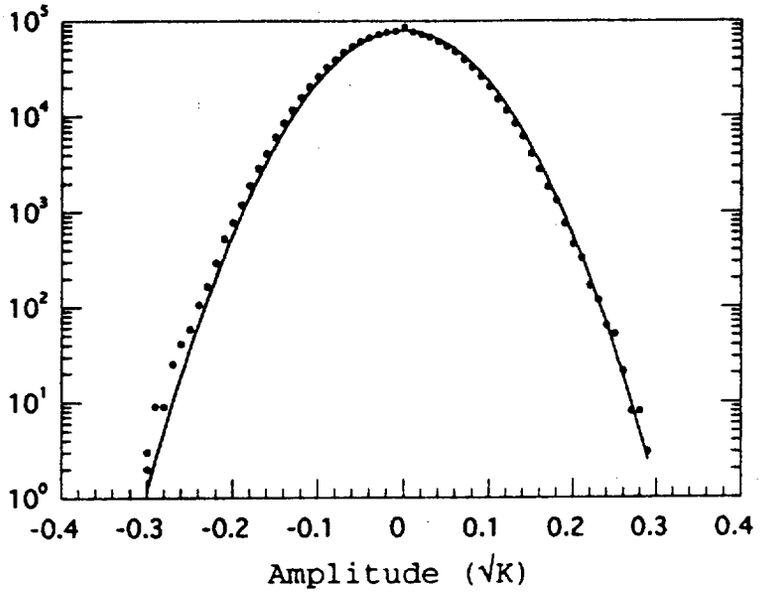

FIG. 8 – Histogram of two hours of data, filtered by the adaptive matched filter. The quantity in the horizontal scale is proportional to the change in the vibration amplitude of the bar, and is reported in units of $K^{1/2}$. The variance of the data expresses the effective temperature of the detector T_{eff}=4.1 mK.

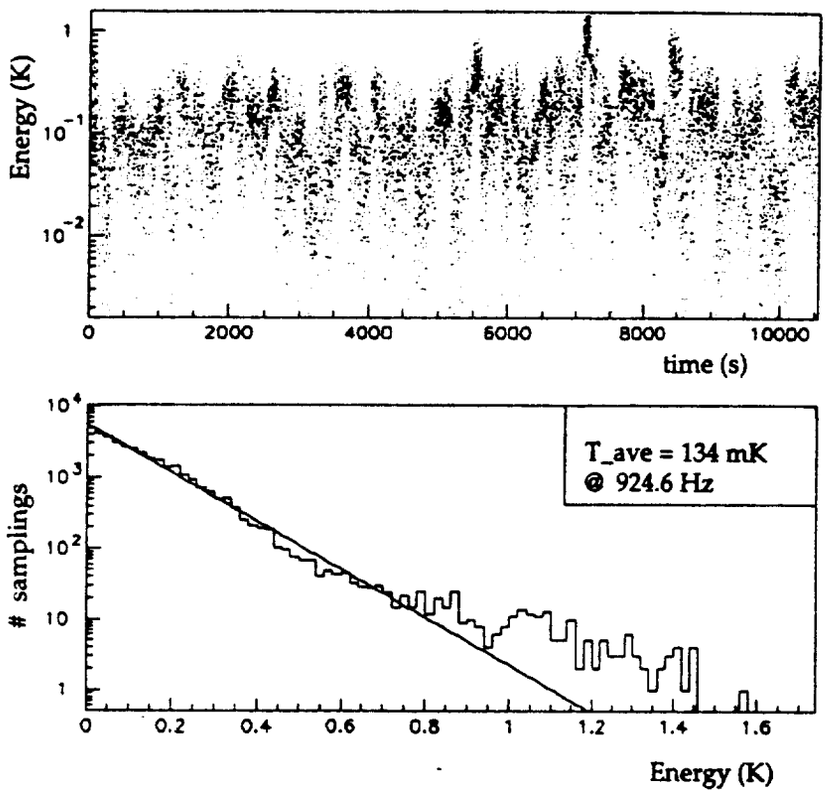

FIG. 9 – Measurement of the Brownian noise: a) history and b) distribution of the vibration energy of the + mode in a three hours period. The average energy is in agreement with the thermodynamic temperature of the bar.